the table would be increased by the cratic entropy $S_c = R \ln 55$ (= 33 J/K mol) and make ΔG more negative by 10 kJ/mol. Because we doubt[9] whether it is correct to replace a translational entropy by a mixing entropy, such as S_c, this correction was not applied.
(8) R. W. Gurney, "Ionic Processes in Solution", McGraw-Hill, New York, N.Y., 1953.
(9) G. Schwarzenbach, *Pure Appl. Chem.*, **24**, 307 (1970).
(10) D. J. Haas, D. R. Harris, and H. H. Miller, *Acta Crystallogr.*, **19**, 676 (1965).
(11) M. Eigen, *Angew. Chem.*, **75**, 489 (1963).

Thermal and Nonthermal Decompositions, Eliminative Ionic Polymerization, and Negative Temperature Coefficients in the i-C_4H_{10}–Benzyl Acetate System. A Time-Resolved Chemical Ionization Mass Spectrometric Study

M. Meot-Ner (Mautner),* E. P. Hunter, and F. H. Field

Contribution from the Rockefeller University, New York, New York 10021.

Received January 20, 1977

Abstract: The i-C_4H_{10}–benzyl acetate (BzOAc) reaction system was investigated by pulsed, time-resolved chemical ionization mass spectrometry. The following novel observations were made: (a) The rate constant, k_f, for i-C_4H_{10} + BzOAc → products decreases from 24×10^{-10} at 320 K to 0.61×10^{-10} cm^3/mol s at 520 K, with a negative temperature dependence of $k_f \propto T^{-6}$–T^{-10}. (b) The Bz^+ and $BzOAcH^+$ ions are formed from the competitive fast decomposition of $(t\text{-}C_4H_9{}^+\cdot BzOAc)^*$; the difference between the activation energies for the two processes is 13.6 kcal/mol. (c) The Bz^+ ion initiates a sequence of eliminative ionic polymerization reactions of the general form $(C_7H_7\cdot(n-1)C_7H_6)^+ + BzOAc \rightarrow (C_7H_7\cdot nC_7H_6)^+ + HOAc$ (n = 0–4). The process appears to proceed at about collision rate and without an activation energy. (d) The polymer ions $(C_7H_7\cdot C_7H_6)^+$, $(C_7H_7\cdot 2C_7H_6)^+$, and $(C_7H_7\cdot 3C_7H_6)^+$ undergo thermal decomposition with the loss of H_2, possibly to form protonated anthracene ions. These reactions are in competition with further polymerization. The rate constant for thermal H_2 loss, $(C_7H_7\cdot C_7H_6)^+ \rightarrow C_{14}H_{11}{}^+ + H_2$, at 470 K is 1.3×10^4 s^{-1}. (e) The $C_7H_7{}^+$ ion formed from BzOAc in CH_4 protonates BzOAc; that formed in i-C_4H_{10} does not. (f) The thermodynamic values for $BzOAcH^+ + BzOAc \rightarrow (BzOAc)_2H^+$ are $\Delta H^\circ = -28.9$ kcal/mol, $\Delta S^\circ = -34.7$ eu. (g) Continuous ionization CIMS appears to correspond to ions formed in 5–15 μs reaction time. (h) Analytical chemical ionization experiments using i-C_4H_{10} should be performed at the lowest temperature compatible with other experimental requirements.

Since the introduction of chemical ionization mass spectrometry (CIMS) about a decade ago,[1,2] the technique has been applied to the analysis of a large variety of substances. Despite the widespread application, the mechanism and kinetics of the processes leading to the observed CIMS spectra of complex molecules have scarcely been investigated. One of the earlier attempts to make such an investigation was directed at the examination of temperature and pressure effects in the i-C_4H_{10} CIMS spectra of benzyl acetate (BzOAc) and related compounds.[3-6] The most significant ions observed in the i-C_4H_{10}–BzOAc system were Bz^+($C_7H_7{}^+$, *m/e* 91), $BzOAcH^+$ (*m/e* 151), $(BzOAc)_2H^+$ (*m/e* 301), $Bz^+\cdot BzOAc$ (*m/e* 241), and $Bz^+\cdot BzOAc\text{-}HOAc$ (*m/e* 181). The kinetic studies were directed mostly at the formation of the Bz^+ fragment ion and MH^+–HOAc fragment ions in other acetates. In that work, which was done in this laboratory using a conventional continuous ionization technique, it was assumed that ions are formed in the ion source in a thin ribbon at the level of the entrance of the ionizing electron beam to the ion source. These ions were then assumed to undergo chemical reactions while diffusing from the ionization area to the ion exit slit. The reaction sequence of major interest was assumed to be the formation of protonated quasi-molecular ions (MH^+) by proton transfer from t-$C_4H_9{}^+$ to the additive molecules, followed by the thermal decomposition of the MH^+ ions.

Following the introduction of pulsed ionization technique in our laboratory, we undertook to reexamine the mechanism of reactions in the i-C_4H_{10}–BzOAc system. As will be seen, the results require us to modify our idea about the mechanism of the formation of the protonated molecular ion and the fragment ions; they lead to the observation of previously unobserved reactions; and they yield more reliable measurements of rate and equilibrium constants for the principal reactions in this CIMS system. Thus the results illustrate the use of the pulsed technique to clarify the mechanisms of complex CIMS processes.

Experimental Section

The present work was conducted on the Rockefeller University chemical physics mass spectrometer used in the pulsed mode.[7,8] The important feature of this technique is that ions are generated by a short pulse of ionizing electrons, usually of 8–20-μs duration in this work, and the intensities of the ions issuing from the source are recorded explicitly as a function of the residence times (i.e., reaction times) of the ions in the ionization chamber. Assumptions about the spatial distribution of initial ionization and about ion residence times, which were required in the previous work with continuous ionization, are not necessary, and the change of ion intensities with reaction time is directly observable.

Mixtures of benzyl acetate (BzOAc) in i-C_4H_{10} or CH_4 were prepared in a heated bulb, and the mixture was allowed to flow into the source in a stream of additional reactant gas. The technique was described in a previous publication.[3] Usually 1–50 μL of BzOAc was used, leading to a partial pressure of 0.15–7.5 mTorr of BzOAc in 0.5–1.0 Torr of reactant gas in the source. Materials used in this study were benzyl acetate and 2,6-dimethylaniline, MCB, purity >99%; isobutane, Matheson, instrumental grade; methane, Matheson, ultra high purity grade.

Results and Discussions

1. Time-Resolved CIMS of the i-C_4H_{10}–BzOAc System. Examples of time-resolved CIMS in the i-C_4H_{10}–BzOAc

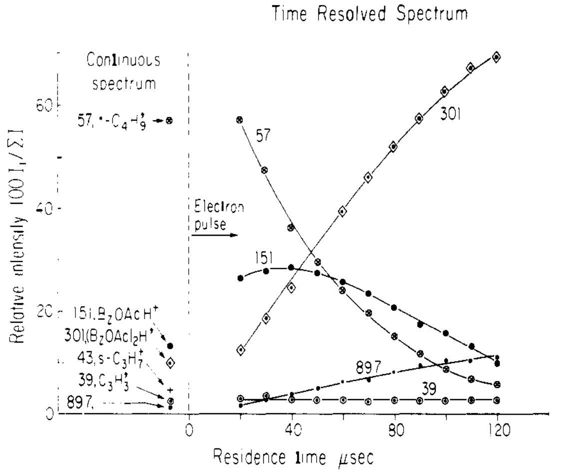

Figure 1. Temporal ion profiles and continuous ionization mass spectrum in the i-C_4H_{10}-BzOAc system at 362 K, $P_{total} = 0.78$ and $P_{BzOAc} = 0.67 \times 10^{-3}$ Torr.

system will be discussed and compared with continuous CIMS in this section. Individual reactions of interest will be discussed in following sections.

An example of the time-ion intensity profiles in the i-C_4H_{10}-BzOAc system at the relatively low temperature of 362 K at a total pressure of 0.78 Torr and partial pressure of BzOAc of 0.67×10^{-3} Torr is shown in Figure 1.

The major feature of the system is the decay of the t-$C_4H_9^+$ ions and the formation of $BzOAcH^+$ (*m/e* 151) with the subsequent formation of $(BzOAc)_2H^+$ (*m/e* 301). The intensity of $BzOAcH^+$ goes through a maximum, which is characteristic of an intermediate in a series of consecutive reactions.

In Figure 1 we observe a metastable ion at *m/e* 89.7, with a time profile parallel to that of the $(BzOAc)_2H^+$ (*m/e* 301) ion; a similar relation between $I_{89.7}$ and I_{301} is observed also in Figure 2. In pressure studies aimed at clarifying the origin of this metastable we observed that the intensity ratio $I_{89.7}/I_{301}$ increased with increasing source pressure, in particular above 1 Torr. We also noted that the shape of the metastable peak broadened and the position of the maximum shifted between *m/e* 89.5 and 90.5 as the field strength between our ion exit slit and the focusing electrodes was varied between 50 and 950 V/cm. These observations suggest that this metastable is the product of a collisionally induced dissociation of the $(BzOAc)_2H^+$ dimer ion outside the ion exit slit.

As for the major reactant ions apart from t-$C_4H_9^+$, the $C_3H_7^+$ ion (*m/e* 43) is not observed once the ionizing beam has ended (after about 20 µs). This is due to the fast disappearance of $C_3H_7^+$ in the reaction $C_3H_7^+ + i\text{-}C_4H_{10} \rightarrow C_3H_8 + t\text{-}C_4H_9^+$. On the other hand, the stable $C_3H_3^+$ ion (*m/e* 39) does not react with any component of the system, and its intensity remains a constant fraction of the total ion current during observable reaction times.

Figure 2 illustrates the time-resolved spectrum of the i-C_4H_{10}-BzOAc system at a higher temperature and BzOAc concentration than those in Figure 1, i.e., 470 K and 11.9×10^{-3} Torr. This spectrum is quite complex, and is dominated at low residence times by the Bz^+ ion (*m/e* 91) and at long residence times by a set of ions which are products of the reaction of Bz^+ with BzOAc. These are ions formed by condensation reactions with elimination of HOAc, namely, $C_{14}H_{13}^+$ ($C_7H_7 \cdot C_7H_6^+$), *m/e* 181; $C_{21}H_{19}^+$ ($C_7H_7 \cdot (C_7H_6)_2)^+$, *m/e* 271; $C_{28}H_{25}^+$ ($C_7H_7 \cdot (C_7H_6)_3)^+$, *m/e* 361; and $C_{35}H_{31}^+$ ($C_7H_7 \cdot (C_7H_6)_4)^+$, *m/e* 451 (not shown on Figure 2). Another set of ions are formed by loss of H_2 from the above ions, i.e., $C_{14}H_{13}^+ \rightarrow C_{14}H_{11}^+$ (*m/e* 179) + H_2; $C_{21}H_{19}^+ \rightarrow C_{21}H_{17}^+$ (*m/e* 269) + H_2; and $C_{28}H_{25}^+ \rightarrow C_{28}H_{23}^+$ (*m/e* 361) + H_2. The reactions occurring were deduced from the stoichiometric information provided by *m/e* values and from the temporal variations of the ionic intensities. A more detailed discussion of the reactions will be given later in the paper. In addition, a continuous ionization i-C_4H_{10} CIMS spectrum was obtained of p-fluorobenzyl acetate, and this exhibited condensation ions containing fluorine atoms. The number of F atoms was seen to be equal to the number of C_7 residues in the ion, and this information constituted a confirmation of the stoichiometry and the postulated structure of the condensation ions formed in benzyl acetate.

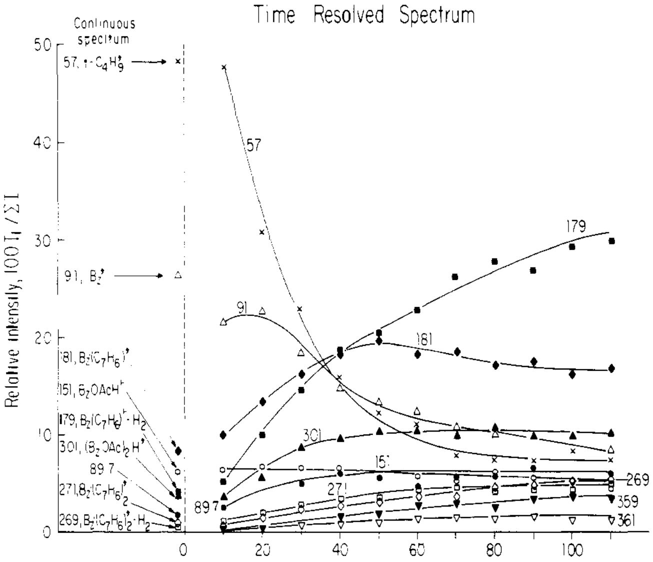

Figure 2. Temporal ion profiles and continuous ionization mass spectrum in the i-C_4H_{10}–BzOAc system at 470 K, $P_{total} = 0.80$ and $P_{BzOAc} = 11.9 \times 10^{-3}$ Torr.

For convenience, the group of ions generated from Bz^+, i.e., *m/e* 91, 181, 179, 271, 269, 361, and 359, will be referred to as the Bz^+ group ions; the ions 151, 301, and 89.7 as the $BzOAcH^+$ ions. The sum of ion intensities in these groups will be referred to as $\{Bz^+\}$ and $\{BzOAcH^+\}$.

Since the $C_7H_7^+$ ion is generated as a decomposition product of BzOAc in a relatively low-energy system, we consider it to be the benzyl ion, Bz^+. This ion has been shown to have a lifetime $>10^{-5}$ s in the gas phase.[9] Other structures or a mixture of structures is also possible, and in fact are indicated to exist in the CH_4-BzOAc system, as will be shown later.

A schematic representation for reactions in the i-C_4H_{10}-BzOAc system that can account for the ion profiles observed in Figures 1 and 2 is given in Scheme I. A detailed justification for this scheme of reactions, based on ion intensity ratios as a function of reaction time (Figure 3) and other kinetic arguments, and further discussion of the reactions shown in it will be given in the sections to follow. Rate constants for some of the reactions are summarized in Table I.

2. Kinetics of the Reaction t-$C_4H_9^+$ + BzOAc $\xrightarrow{k_f}$ Products: The Negative Temperature Dependence of k_f. The rate constant, k_f, for the overall reaction t-$C_4H_9^+$ + BzOAc → products can be found from the rate of disappearance of the t-$C_4H_9^+$ ion. For example, rate constants obtained at three temperatures from the slopes of plots of ln ($I_{57}^+/\Sigma I$) vs. time give $k_f^{323} = 24 \times 10^{-10}$, $k_f^{440} = 2.8 \times 10^{-10}$, and $k_f^{520} = 0.61 \times 10^{-10}$ cm^3/mol s. The calculated collision rate between t-$C_4H_9^+$ and BzOAc is 17×10^{-10} cm^3/mol s. Thus the collision efficiency for the H^+ transfer reaction decreases from about unity at 320 K to 0.035 at 520 K.

The temperature dependence of k_f, in the form of ln k_f vs. ln T, is shown in Figure 4. The magnitude of the negative

Scheme I

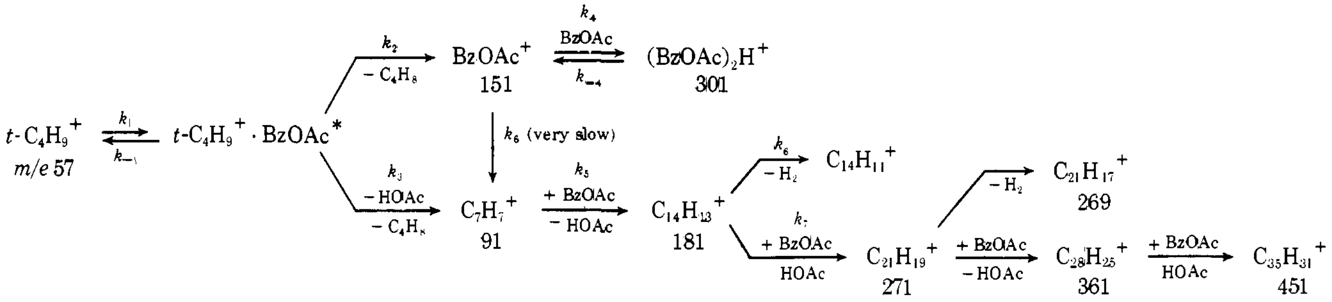

temperature coefficient can be expressed approximately as $k_f \propto T^{-6}$ at the lower temperature range and $k_f \propto T^{-10}$ at the higher temperature range. Alternatively, a function of the form $k_f = CT^{-n} \exp(-E_a/RT)$, with $n = 12 \pm 2$, $E_a = 3 \pm 2$ kcal/mol would also describe the experimental temperature dependence of k_f, as shown by the broken line in Figure 4. Thus the curvature of the experimental plot in Figure 4 may indicate the presence of small activation energy, largely overwhelmed by a large negative preexponential temperature coefficient.

A pressure study, indicated by the points in the box in Figure 4, shows that the reaction t-$C_4H_9^+$ + BzOAc → products is, as expected, second order, i.e., first order in both t-$C_4H_9^+$ and BzOAc. It is of much interest that we observe a large negative temperature dependence for this bimolecular proton transfer reaction. Although we did observe significant negative temperature coefficients for bimolecular hydride ion transfer reactions,[7,10] all ion-molecule proton transfer reactions whose temperature coefficients were measured to date displayed zero or very small temperature dependence.[11]

It is conceivable that the negative temperature dependence in the present H^+ transfer reaction would originate from the complexity of the reactants, or from the fact that substantial rearrangement, probably including a cyclic intermediate, is required for proton transfer in the reaction complex (see Scheme III). To check whether the complexity of the reactant accounts for the negative temperature dependence, we measured the rate constant for an H^+ transfer reaction in a system of comparable complexity, t-$C_4H_9^+$ + 2,6-$(CH_3)_2C_6H_4NH_2$ → 2,6-$(CH_3)_2C_6H_4NH_3^+$ + C_4H_8. We found that at 368 K $k_f = 10 \pm 3$; at 475 K $k_f = 15 \pm 3$; and at 560 K $k_f = (15 \pm 3) \times 10^{-10}$ cm^3/mol s. Thus, this reaction proceeds at about collision rate, without a significant temperature dependence. Of course, the reaction involving BzOAc is less exothermic than that of the amine, which may account for the difference in behavior of the two reactions.

3. Kinetics of the Reaction t-$C_4H_9^+$ + BzOAc → Products: The Mechanism of the Formation of BzOAcH$^+$ and Bz$^+$. The mechanism of formation of the $C_7H_7^+$ fragment ion is a question of major interest in the present system. As noted earlier, in previous work it was assumed that it is formed by the thermal decomposition of BzOAcH$^+$, i.e., Scheme II.

Scheme II

$$t\text{-}C_4H_9^+ + \mathrm{BzOAc} \rightarrow \mathrm{BzOAcH}^{+*} \xrightarrow{M} \mathrm{BzOAcH}^+ \text{ (thermal)}$$

$$\xrightarrow[k_d]{?} \mathrm{Bz}^+ + \mathrm{HOAc}$$

If this sequence occurs the sum of intensities in the {BzOAcH$^+$} group of ions should decrease with increasing reaction time, with an equal increase in the sum of intensities of the {Bz$^+$} group ions. The examination of Figure 2 and Figure 3a shows that such a change is indeed observed, but at a rather slow rate; i.e., the intensity ratio {Bz$^+$}/{BzOAcH$^+$} increases only by 15% in 100-μs reaction time. It is clear that this process must be very slow, with a half-life of several hundred microseconds. In Figure 2 we observe a decrease of ≈40% in the intensity of i-$C_4H_9^+$ in 50-μs reaction time. If Scheme II were correct, with $1/k_d > 100$ μs, we would observe a corresponding increase in BzOAcH$^+$ in this time, i.e., the BzOAcH$^+$ ions would be formed and would not decompose in the first 50 μs. However, we observe an increase in the m/e 91, 181, and 179 ion intensities simultaneous with the disappearance of t-$C_4H_9^+$ in the first 50 μs. From these observations it is obvious that the major mechanism for the formation of Bz$^+$ is not the slow thermal decomposition of BzOAcH$^+$. Rather, we think the data support the hypothesis that Bz$^+$ and BzOAcH$^+$ are competitive products of the reaction t-$C_4H_9^+$ + BzOAc → products, as shown in Scheme I, with the ratio Bz$^+$/BzOAcH$^+$ = k_3/k_2 increasing with increasing temperature. We note that the

Table I. Rate Constants and Thermodynamic Values Measured in the i-C_4H_{10} + BzOAc and CH_4 + BzOAc Reaction Systems

Reaction	Temp, K	Quantity measured	Result
$t\text{-}C_4H_9^+ + \mathrm{BzOAc} \xrightarrow{k_f} \text{products } (\mathrm{BzOAcH}^+ \text{ and } \mathrm{Bz}^+)$	323	k_f	24×10^{-10} cm^3/mol s
	440		2.8×10^{-10}
	520		0.61×10^{-10}
$C_7H_7^+ + \mathrm{BzOAc} \xrightarrow{k_5} C_7H_7(C_7H_6)^+ + \mathrm{HOAc}$	410	k_5	7.1×10^{-10}
	520		4.6×10^{-10}
	572		2.3×10^{-10}
$C_7H_7(C_7H_6)^+ \xrightarrow{k_6} C_{14}H_{11}^+ + H_2$	470	k_6	1.3×10^4 sec^{-1}
$\mathrm{BzOAcH}^+ + \mathrm{BzOAc} \overset{k_4}{\rightleftarrows} (\mathrm{BzOAc})_2\mathrm{H}^+$	360	k_4	28×10^{-10} cm^3/mol s
		$\Delta H°$	−28.9 kcal/mol
		$\Delta S°$	−34.7 cal/deg mol

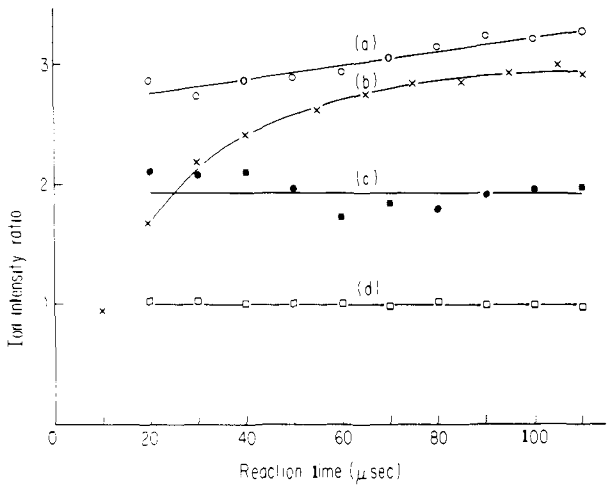

Figure 3. Ion intensity ratios in the i-C_4H_{10}–BzOAc system of Figure 2 as a function of reaction time: (a) $\{Bz^+\}/\{BzOAcH^+\}$, i.e., $(I_{91} + I_{181} + I_{179} + I_{271} + I_{269} + I_{361} + I_{359})/(I_{151} + I_{301} + I_{89.7})$; (b) $(I_{301} + I_{89.7})/I_{151}$; (c) $I_{179}/(I_{271} + I_{269} + I_{361} + I_{359})$; (d) $I_{269}/(I_{361} + I_{359})$.

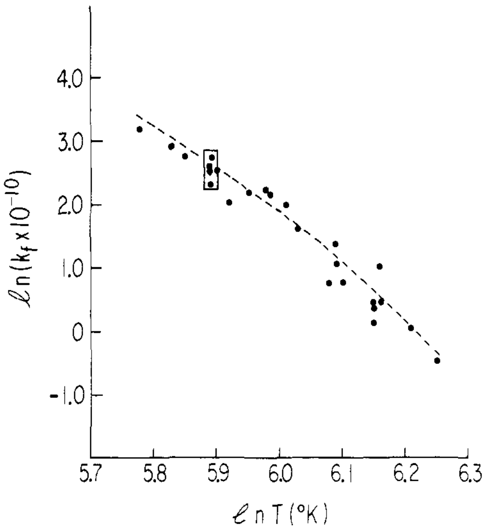

Figure 4. Temperature dependence of the rate constant, k_f, for t-$C_4H_9^+$ + BzOAc (k_f) → products. Solid line is drawn through experimental points; broken line is for $k_{calcd} = CT^{-12}\exp(-3000/RT)$, with C chosen such as to make $\ln k_{calcd} = \ln k_f$ at $\ln T = 6.0$. Points within box indicate a pressure study to show that k_f is independent of P_{BzOAc}. These points were obtained at values of $P_{total} = 0.78$ Torr, $P_{BzOAc} = 0.22, 0.44, 0.67$, and 1.5 mTorr.

structures of the ions shown in Scheme III and elsewhere are not known, and represent only some plausible possibilities.

Alternatively, the following sequence could occur (Scheme IV). If Scheme IV were operative the ratio of $\{BzOAcH^+\}/\{Bz^+\}$ would be proportional to the pressure of i-C_4H_{10}. We tested this possibility in a reaction system at 470 K with $P_{BzOAc} = 9.0 \times 10^{-3}$ Torr and $P_{i\text{-}C_4H_{10}} = 0.4$–$1.5$ Torr. We found that the ratio of the sum of the ions in the $BzOAcH^+$ group to the sum of the ions in the Bz^+ group is independent of the i-C_4H_{10} pressure (Figure 5). Thus Scheme IV does not seem to be correct, and the formation of Bz^+ appears to be due to the competitive decomposition of t-$C_4H_9^+$·BzOAc* to form Bz^+ or $BzOAcH^+$, as shown in Schemes I and III. Assuming that Scheme III is operative, it is possible to get a measure for the relative activation energies and preexponential factors of k_2 and k_3 from the temperature dependence of $\{Bz^+\}/\{BzOAcH^+\}$. This treatment is not rigorously correct, since t-$C_4H_9^+$·BzOAc* is probably not a thermalized population, but the approximate results are still of interest. A plot of $\{Bz^+\}/\{BzOAcH^+\}$ vs. $10^3/T$ is shown in Figure 6. We assume

$$\frac{\{Bz^+\}}{\{BzOAcH^+\}} = \frac{k_3}{k_2} = \frac{A_3}{A_2}e^{-(Ea_3 - Ea_2)/RT}$$

From the plot of Figure 6 we obtain $Ea_3 - Ea_2 = 13.6$ kcal/mol. It has been shown[3] that a difference of this magnitude between the activation energies is compatible with the difference between the $\Delta H°$ values for these reactions. Also from Figure 6 we obtain: $\log A_3 - \log A_2 = 6.7$. The reaction intermediate associated with k_2 (Scheme III) is highly constrained and of low entropy, and thus this result is reasonable.

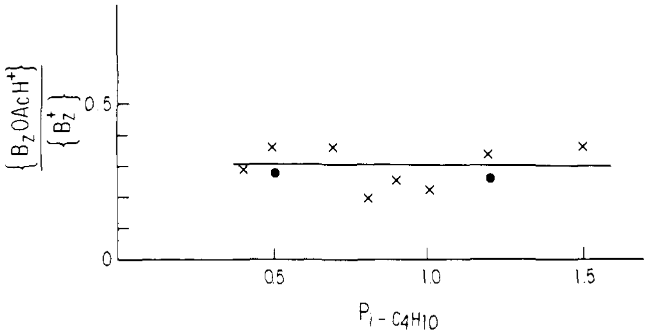

Figure 5. A plot that demonstrates the relative rates of formation of $BzOAcH^+$ vs. Bz^+ ions (obtained from the ratio of ion intensities in the $\{BzOAcH^+\}/\{Bz^+\}$ groups) is independent of i-C_4H_{10} pressure: ×, points obtained by continuous ionization; ●, check points obtained by the time-resolved technique. $T = 470$ K, $P_{BzOAc} = 9.0 \times 10^{-3}$ Torr.

4. Reactions of Bz^+ ($C_7H_7^+$) and Its Product Ions: Eliminative Polymerization and Thermal H_2 Loss. As we note in

Scheme III

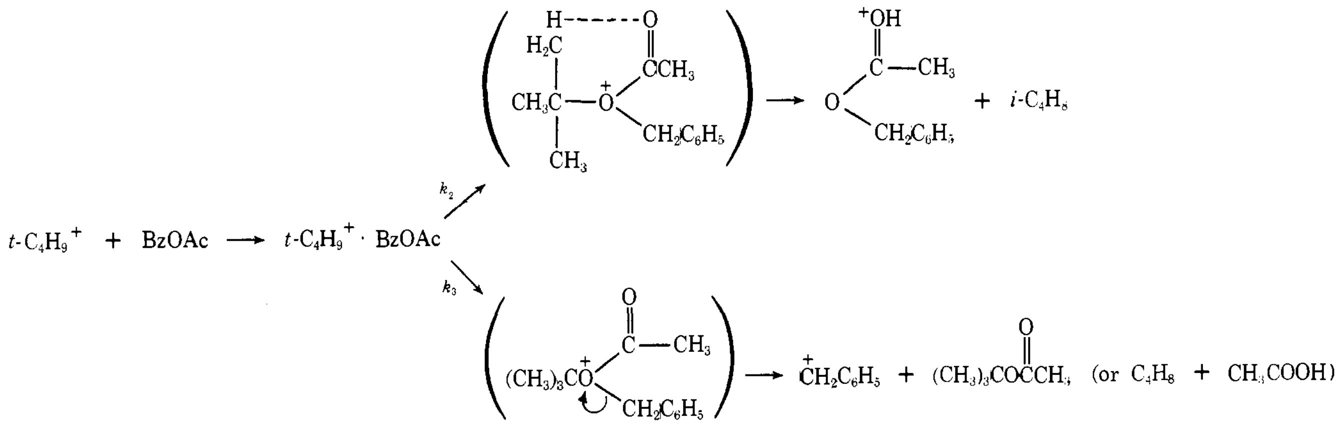

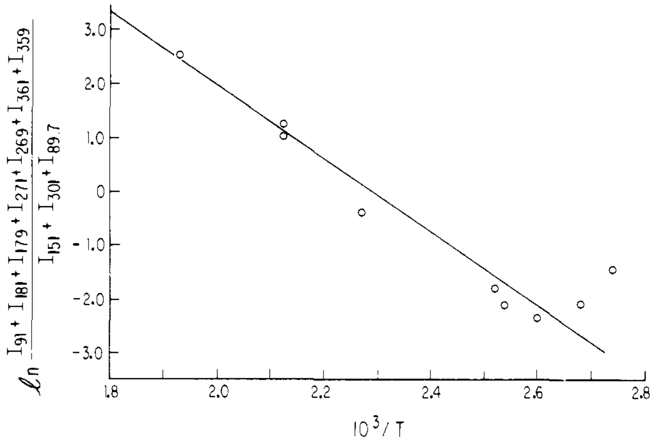

Figure 6. Arrhenius-type plot for the relative rates of formation of Bz^+ vs. $BzOAcH^+$ as a function of the temperature.

Scheme IV

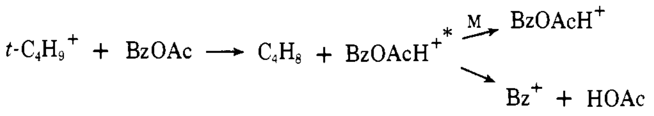

Scheme V

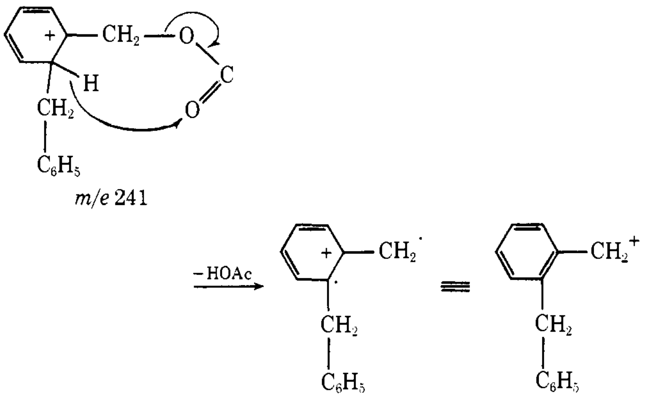

Scheme I, Bz^+ formed as a fragment ion in the i-C_4H_{10} + BzOAc system leads to a sequence of reactions which can be characterized as eliminative ionic polymerization with the loss of an HOAc molecule in each step. The general formula is: $A^+ + BzOAc \rightarrow (A + C_7H_6)^+ + HOAc$. The ions that we observe in this series are $C_7H_7^+$ (*m/e* 91), $C_{14}H_{13}^+$ (*m/e* 181), $C_{21}H_{19}^+$ (*m/e* 271), $C_{28}H_{25}^+$ (*m/e* 361), and $C_{35}H_{31}^+$ (*m/e* 451). The last ion is only observed under continuous ionization, i.e., high sensitivity conditions, at very high concentrations of BzOAc. This sequence of reactions also branches, with H_2 loss reactions, to give the *m/e* 181 − 2 = 179 ion, which is the major reaction product in Figure 2; the *m/e* 271 − 2 = 269 ion and the *m/e* 361 − 2 = 359 ions are also seen.

Eliminative gaseous ionic polymerization is an unusual and novel type of reaction, and we investigated the kinetics of some of these processes. The first step in the process is the reaction $C_7H_7^+ + BzOAc \rightarrow C_{14}H_{13}^+ + HOAc$ (k_5). A plausible mechanism for the displacement of HOAc from BzOAc by $C_7H_7^+$ involves the intermediate (*m/e* 241), as shown in Scheme V.

It might be expected that this process would require a significant activation energy. To examine this, we measured k_5 at a range of temperatures, and observed $k_5^{410} = 7.1 \times 10^{-10}$, $k_5^{480} = 3.6 \times 10^{-10}$, $k_5^{520} = 4.6 \times 10^{-10}$, and $k_5^{572} = 2.3 \times 10^{-10}$ cm³/mol s. Some scattering of the data and possibly a small negative temperature dependence is seen, but no significant activation energy is present. This indicates that the energy released upon the formation of the $Bz^+ \cdot BzOAc$ complex into the internal degrees of freedom is sufficient to overcome the energy barrier for this reaction.

Scheme VI

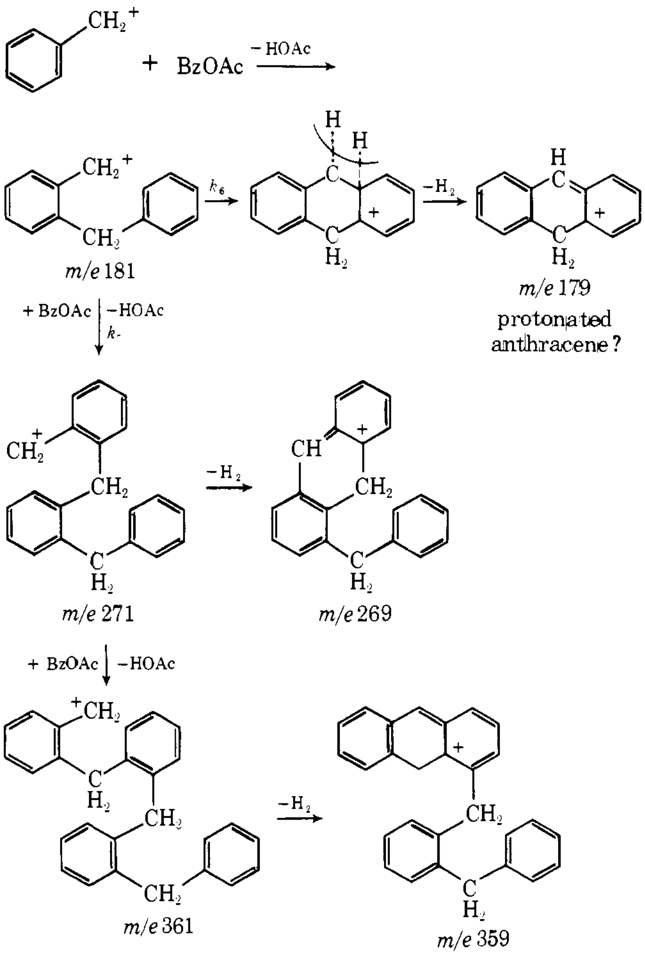

If the *m/e* 181 ion indeed possesses the ortho structure as shown in Scheme V, then the consequent formation of the *m/e* 179 ion can be seen as cyclization with H_2 loss, leading probably to a protonated anthracene ion (Scheme VI). This process is apparently in competition with reaction 7, which leads to higher mass products. If reactions 6 and 7 are indeed competitive processes, then the ratio of the products of these reactions should be $I_{179}/(I_{271} + I_{269} + I_{371} + I_{359}) = k_6/k_7$ = constant (with respect to time). The independence of this ion intensity ratio on reaction time is indeed observed (Figure 3c). Likewise, the independence of $I_{269}/(I_{361} + I_{359})$ on reaction time (Figure 3d) shows that ions 269 and 361 are formed as products of competitive reactions (H_2 loss and eliminative polymerization) of ion 271.

As we have just shown, ion intensity ratio considerations indicate that the *m/e* 179 ion is formed in competition with *m/e* 271. In Schemes I and VI we postulate that 179 is formed by a unimolecular reaction of the *m/e* 181 ion, while 271 is the product of a bimolecular reaction of this ion with BzOAc. This mechanism suggests that $(I_{271} + I_{261} + I_{361} + I_{359})/I_{179}$ should be proportional to P_{BzOAc}. This relation is indeed observed (Figure 7). The kinetic data is thus completely consistent with the reaction sequence of Scheme I, which shows a process of eliminative polymerization to form $C_7H_7 \cdot (C_7H_6)_n{}^+$, where each polymerization step is also in competition with H_2 elimination from the ionic precursor of that step.

The observation of gaseous ionic polymerization in benzyl acetate motivated us to check whether such a process may occur also in the condensed phase upon the protonation of

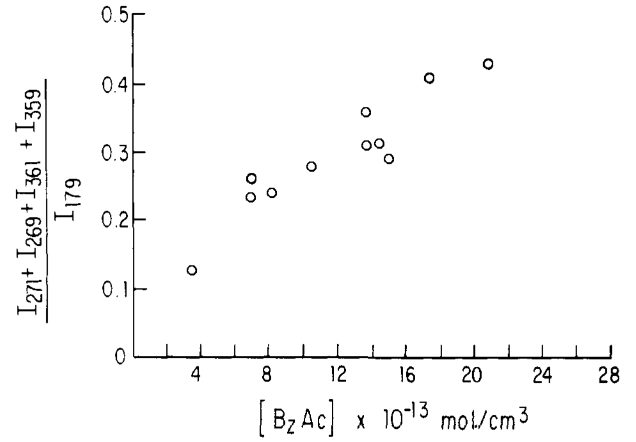

Figure 7. Intensity ratio of the sum of the m/e 271 ion and higher products formed therefrom vs. the m/e 179 ion, as a function of the density of BzAOc in the ion source. Experimental conditions: T = 470 K, $P_{i-C_4H_{10}}$ = 0.80 Torr.

BzOAc. Indeed, upon the addition of concentrated H_2SO_4 to BzOAc we observed the formation of a brown polymer from which a white gluey material separated out upon further contact with the BzOAc–H_2SO_2 mixture; this material turned hard and brittle upon the removal of the solvent. The material seemed to melt without decomposition and was soluble in toluene. These results suggest that the material is an oligomer of hydrocarbon units, and it may well be the analogue of the polymer observed in the gas phase. The polymerization seems to depend upon the presence of the benzyl moiety, for neither phenyl acetate nor *tert*-butyl acetate exhibited any reaction when mixed with H_2SO_4. No condensation has been observed in the gas phase with these acetates, and we thus observe a parallelism between the tendency to polymerize in the gas and condensed phases in these acetates.

The time dependence of the ion intensities in the i-C_4H_{10}–BzOAc system and knowledge of the reaction sequence in Scheme I can be used to obtain further quantitative information on this reaction system. In particular, we wish to calculate the rate constant for H_2 loss from $C_{14}H_{13}^+$ (m/e 181) and to show that this is indeed a thermally activated process. From the rate of disappearance of the t-$C_4H_9^+$ ion in Figure 2 and the known concentration of BzOAc we can calculate a value of 2.2×10^4 s^{-1} for the quantity $(k_f{}^2 + k_f{}^3)$ (BzOAc), where the k_f are rate constants in the reaction

$$t\text{-}C_4H_9^+ + \text{BzOAc} \begin{cases} \xrightarrow{k_f{}^3} \text{Bz}^+ + \text{neutrals} \\ \xrightarrow{k_f{}^2} \text{BzOAcH}^+ + \text{neutrals} \end{cases}$$

The branching ratio, $k_f{}^3/k_f{}^2 = \{Bz^+\}/\{BzOAcH^+\}$, may be observed from Figure 3a to be 2.8; therefore the rate of formation of Bz^+, $k_f{}^3$, is 1.6×10^4 s^{-1}. It can be shown[12] that in the sequential reaction A (k_a) → B (k_b) → C the following relation holds: $k_a/k_b = (B)_m/(A)$ where $(B)_m$ is the maximum concentration of B as a function of reaction time and (A) is the corresponding concentration of A. Thus we may write $k_f{}^3/k_5(\text{BzOAc}) = (I_{91})_m/I_{57}$, and the experimental value of this ratio from Figure 2 is 0.70. Since $k_f{}^3 = 1.6 \times 10^4$ s^{-1}, we find that the rate of formation of 181^+, i.e., k_5(BzOAc), is 2.3×10^4 s^{-1}. To find the rate of disappearance of the m/e 181 ion the same procedure is used, and we write $k_5(\text{BzOAc})/(k_6 + k_7(\text{BzOAc})) = (I_{181})_m/I_{91}$, the value of which may be obtained from Figure 2 as 1.3. Thus $(k_6 + k_7(\text{BzOAc})) = 1.8 \times 10^4$ s^{-1}. The ratio $k_6/k_7(\text{BzOAc}) = 1.9$ is found from the ratio of the products of the parallel reaction in which the m/e 181 ion disappears. From the two expressions containing k_6 and k_7 a value for k_6 can be calculated. Consequently, the total calculation gives the result that for the reaction $C_{14}H_{13}^+$ (k_6) → $C_{14}H_{11}^+ + H_2$, the value of k_6 is 1.1×10^4 s^{-1}. This rate constant corresponds to a half-life of the $C_{14}H_{13}^+$ ions of 54 μs. During this time each $C_{14}H_{13}^+$ ion undergoes about 900 collisions with i-C_4H_{10} molecules; this is surely sufficient to yield a thermal population of these ions. We thus conclude that the elimination of H_2 from this ion is indeed a thermally activated decomposition process.

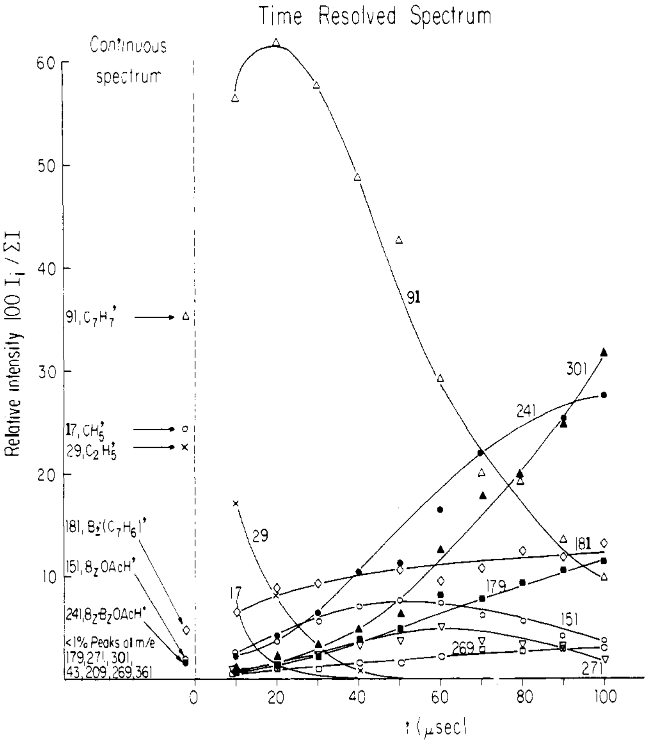

Figure 8. Time resolved and continuous ionization mass spectrum of the CH_4–BzOAc system at 360 K, P_{total} = 0.80 and $P_{BzOAc} = 1.2 \times 10^{-3}$ Torr.

5. The CH_4–BzOAc System. Time-resolved and continuous mass spectra of the CH_4–BzOAc system at 360 K are shown in Figure 8. Compared with the i-C_4H_{10}–BzOAc system at the same temperature (Figure 1), we observe that while in i-C_4H_{10} at 360 K no $C_7H_7^+$ fragment is observed, it is the predominant ion in CH_4. Increased fragment formation in CH_4 vs. i-C_4H_{10} CIMS is commonly observed and is related to the exothermicity of proton transfer from CH_5^+ and $C_2H_5^+$ to BzOAc.

The major reaction in the CH_4–BzOAc system in Figure 8 is the disappearance of the $C_7H_7^+$ ion with the simultaneous formation of 181^+, 179^+, 241^+, and 301^+ as major products. The first two ions are similar to those observed in the i-C_4H_{10}–BzOAc system as had been discussed before. The ion at m/e 241 is apparently $C_7H_7^+$·BzOAc, which was postulated as an intermediate in Scheme V. Presumably at 360 K its lifetime is long enough to be stabilized by collision with CH_4 molecules. The novel feature of the CH_4–BzOAc system is the formation of the m/e 301 ion with the disappearance of $C_7H_7^+$. As we noted before, the $\{Bz^+\}/\{BzOAcH^+\}$ ratio in the i-C_4H_{10}–BzOAc system is constant or slightly decreasing with reaction time; however, in the CH_4–BzOAc system the $BzOAcH^+$ group is obviously increasing with time. These observations indicate the reaction scheme in the CH_4–BzOAc system as shown in Scheme VII.

The fact that in this system $C_7H_7^+$ can protonate BzOAc indicates that it is not Bz^+, but a higher energy $C_7H_7^+$ isomer. Such an isomer may be formed as a consequence of the high exothermicity (≈70 kcal/mol) of the H^+ transfer from CH_5^+ to BzOAc.

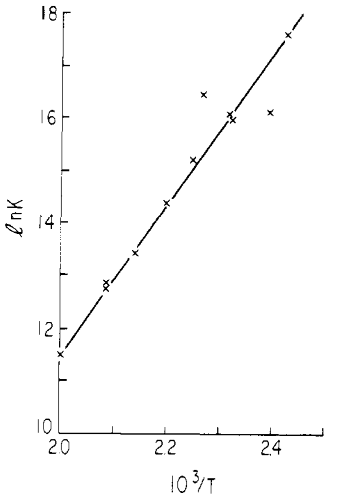

Figure 9. van't Hoff plot for $BzOAcH^+ + BzOAc \rightleftarrows (BzOAc)_2H^+$; $P_{total} = 0.90$ and $P_{BzOAc} = 3.90 \times 10^{-3}$ Torr. Thermodynamic results: $\Delta H° = 28.9$ kcal/mol; $\Delta S° = -34.9$ cal/deg mol.

Scheme VII

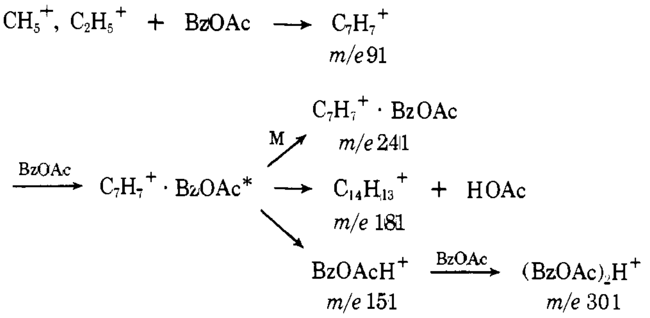

5. The Reaction $BzOAcH^+ + BzOAc \overset{k_4}{\rightleftarrows} (BzOAc)_2H^+$. As noted in Figure 1 the dimer ion $(BzOAc)_2H^+$ (and the corresponding metastable at *m/e* 89.7) is formed rapidly at low temperatures and is observed to be the final product of the ionic reactions under those conditions. At higher temperatures the ratio I_{301}/I_{151} is observed to achieve a finite constant ratio; i.e., the time dependence of the ratio $(I_{301} + I_{89.7})/I_{151}$ becomes essentially constant after 70-μs reaction time (Figure 3b). In pulsed high-pressure mass spectrometric studies of ion-molecule clustering this is usually interpreted to indicate equilibrium in the clustering reaction. The equilibrium constant for the $(BzOAc)_2H^+$ ion formation is written as $K = (I_{301} + I_{89.7})/(I_{151})(P_{BzOAc})$; observations at different temperatures yield a van't Hoff plot as shown in Figure 9. The thermodynamic values obtained from this plot are: $\Delta H° = -28.9$ kcal/mol and $\Delta S° = -34.9$ cal/deg mol. These values for the protonated dimer formation process are similar to those found in other oxygen containing molecules, e.g., $H_3O^+{\cdot}H_2O$, $CH_3OH_2^+{\cdot}CH_3OH$, and $(CH_3)_2OH^+{\cdot}(CH_3)_2O$.[13] Thus it appears that the possibility of bidentate bonding in the acetate dimer, i.e., **1**, does not affect significantly the thermodynamics of the process.

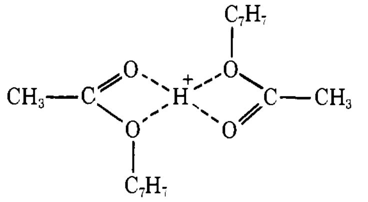

Because of the great complexity of the reaction system it is hard to obtain kinetic data for the association reaction at the higher temperature range. At low temperature, however, the formation of $(BzOAc)_2H^+$ constitutes a system of simple consecutive irreversible reactions

$$t\text{-}C_4H_9^+ \xrightarrow[k_f]{BzOAc} BzOAcH^+ \xrightarrow[k_4]{BzOAc} (BzOAc)_2H^+$$

Under these conditions $k_4 = k_f I_{57}/(I_{151})_m$, where I_{57} and $(I_{151^+})_m$ are the intensities of these ions when (I_{151^+}) goes through a maximum, e.g., at ≈38 μs in Figure 1. k_f is obtained from the rate of disappearance of $t\text{-}C_4H_9^+$, and we find $k_4 = 29 \times 10^{-10}$ cm³/mol s. At 360 K, the collision rate of $BzOAcH^+$ with BzOAc is calculated as 20×10^{-10} cm³/mol s; thus the reaction proceeds at about collision rate at these temperatures; i.e., each $(BzOAc)_2H^{+*}$ complex formed by a collision of $BzOAcH^+$ with BzOAc lives long enough to be stabilized by collision. This result is reasonable when one takes into account the great number of degrees of vibrational freedom in the reactants and the large exothermicity of the reaction.

In our previous work,[3] the ratio I_{301^+}/I_{151^+} obtained from continuous data were assumed to represent the equilibrium ion ratio. From the results given in the present paper it is evident that equilibrium is not reached under continuous ionization conditions (see below), and the thermodynamic values obtained in the continuous study are incorrect.

6. Comparison of Continuous and Time-Resolved Mass Spectra. Figures 1, 2, and 8 show continuous and time-resolved mass spectra of $i\text{-}C_4H_{10}$-BzOAc and CH_4-BzOAc systems. The plots in the time-resolved mass spectra start immediately after the end of the ionizing electron pulse; time zero on these plots is the start of the pulse. From comparison of the continuous and time-resolved spectra it is evident that the ion distributions in the continuous spectra correspond to reaction times earlier than the end of the electron pulse. For example, the continuous intensities correspond to the extrapolation of the time-resolved curves to ~15 μs in Figure 1, and 5-8 μs in Figures 2 and 7.

In our apparatus, the distance between the electron entrance slit to the source and the ion exit slit is 2 mm. Ion diffusion times over this distance under our conditions are usually 30-50 μs.[3] The fact that under continuous ionization conditions we observe spectra corresponding to much shorter reaction times indicates that ionization is taking place not only at the level of electron entrance, but also very close to the ion exit slit, and probably over most of the volume of the gas in the source. This may be due to ionization by fast electrons scattered over the whole volume of gas in the source. The ions formed near the ion exit slit are expected to be collected with greater efficiency than those formed in the depth of the source. This will explain our observations that continuous spectra usually correspond to 5-15-μs reaction times.

7. Implications for Analytical Chemical Ionization Mass Spectrometry. We showed in section 2 that the rate constant for the reaction of $t\text{-}C_4H_9^+$ ion with BzOAc decreased by a factor of approximately 30 as the temperature of the mass spectrometer ion source increased from 323 to 520 K (50-247 °C). The analytical sensitivity of $i\text{-}C_4H_{10}$-CIMS for benzyl acetate will consequently be rather small at about 250 °C, a source temperature which is not particularly high by analytical standards. We have pointed out here and in other work[15] that both the magnitude of ion-molecule rate constants and their temperature coefficients are related to the exothermicities of the reactions, and from the proton affinities given by Yamdagni and Kebarle[16] we estimate that the exothermicity of the proton transfer reaction between $t\text{-}C_4H_9^+$ and BzOAc is about 5 kcal/mol, i.e., a rather small value. In many analytical applications of CIMS the reaction gas is chosen to make the exothermicity of the chemical ionization reaction small to decrease the amount of fragmentation of the sample. Our results here show that the analyst must keep in mind the possibility that with a low exothermicity the sensitivity may be relatively low. Beyond that, to achieve best sensitivity he is advised to operate the mass spectrometer ion source at the lowest temperature that is compatible with the other experimental requirements of the system being investigated.

Acknowledgment. This research was supported in part by a grant from the National Science Foundation.

References and Notes

(1) M. S. B. Munson and F. H. Field, *J. Am. Chem. Soc.*, **88**, 2621 (1966).
(2) F. H. Field, *Acc. Chem. Res.*, **1**, 42 (1968).
(3) F. H. Field, *J. Am. Chem. Soc.*, **91**, 2827, 6334 (1969).
(4) W. A. Laurie and F. H. Field, *J. Am. Chem. Soc.*, **94**, 3359 (1972).
(5) W. A. Laurie and F. H. Field, *J. Phys. Chem.*, **76**, 3917 (1972).
(6) W. A. Laurie and F. H. Field, *J. Am. Chem. Soc.*, **94**, 2913 (1972).
(7) J. J. Solomon, M. Meot-Ner, and F. H. Field, *J. Am. Chem. Soc.*, **96**, 3727 (1974).
(8) M. Meot-Ner, Ph.D. Thesis, The Rockefeller University, New York, N.Y., 1975.
(9) J. L. M. Abboud, W. H. Hehre, and R. W. Taft, *J. Am. Chem. Soc.*, **98**, 6072 (1976).
(10) M. Meot-Ner and F. H. Field, *J. Chem. Phys.*, **64**, 277 (1976).
(11) M. Meot-Ner and F. H. Field, *J. Am. Chem. Soc.*, **97**, 2014 (1975).
(12) N. M. Rodiguin and E. N. Rodiguina, "Consecutive Chemical Reactions", Van Nostrand, Princeton, N.J., 1964, p 87.
(13) E. P. Grimsrud and P. Kebarle, *J. Am. Chem. Soc.*, **95**, 7939 (1973).
(14) M. Meot-Ner and F. H. Field, *J. Am. Chem. Soc.*, **97**, 5339 (1975).
(15) M. Meot-Ner and F. H. Field, "Correlations between Rate, Temperature Dependence, Exothermicity, and Reactant Structure in Slow Ion-Molecule Reactions", Paper presented at Seventh International Conference on Mass Spectrometry, Florence, Italy, Sept 1976.
(16) R. Yamdagni and P. Kebarle, *J. Am. Chem. Soc.*, **98**, 1320 (1976).

Phenylium ($C_6H_5^+$) Ion–Molecule Reactions Studied by Ion Cyclotron Resonance Spectroscopy

Maurizio Speranza, Michael D. Sefcik, Jay M. S. Henis, and Peter P. Gaspar*

Contribution from the Department of Chemistry, Washington University,
Saint Louis, Missouri 63130, the Corporate Research Department,
Monsanto Company, Saint Louis, Missouri 63166, and the Laboratorio di Chimica Nucleare
del Consiglio Nazionale delle Ricerche (CNR), Roma, Italy. *Received December 21, 1976*

Abstract: Ion-assisted dehalogenation reactions of halobenzenes provide a convenient source of phenylium ions. Gas-phase reactions of phenylium ions with hydrogen, alkanes, alkyl halides, alkenes, and arenes have been studied by ion cyclotron resonance spectroscopy. Phenylium ions are strong electrophiles, attacking σ as well as π and nonbonding electrons. The reactivity of phenylium ions has carbenoid characteristics.

While relatively little is known about the gas-phase chemistry of phenylium ions $C_6H_5^+$, the literature indicates a renewal of interest in the electronic structure and reactions of this elusive species.

The formation and reactions of phenylium ions in the liquid phase have been reviewed by Richey and Richey.[1] Such reactions as addition of Lewis bases, addition to π-electron systems, and hydride transfer have been reported for aryl cations in solution. However, a mechanistic ambiguity has plagued the solution experiments; alternative pathways which include as reactive intermediates species other than aryl cations, e.g., free radicals and adducts of nucleophiles to diazonium ions, have proven difficult to exclude. The claim has recently been revived that dediazotization of phenyl diazonium ion produces phenyl cations in solution.[2]

Semiempirical SCF calculations of the INDO type have been carried out for the phenylium and 4-aminophenylium ions.[3,4] A singlet ground state with an empty σ orbital has been predicted on the basis of these calculations for the unsubstituted system and nearly degenerate triplet and singlet lowest states for the 4-aminophenylium ion, with vacancies in π and σ orbitals, respectively. Recent ab initio calculations have been interpreted as supporting the assignment of a singlet ground state for the phenylium ion.[5] Stabilization of an empty σ orbital of substituted phenylium ions via "through-bond" interactions has been studied by extended-Hückel molecular orbital calculations.[6]

In order to explain the discrepancy between the ionization potential of phenyl radicals deduced from appearance potentials of $C_6H_5^+$ (8.80 eV) and the value obtained from direct ionization of the radical (9.2 eV)[7] it has been suggested that the $C_6H_5^+$ ion obtained from halobenzenes by electron impact may not possess the phenylium ion structure. Recently, however, collision activation spectra of substituted toluenes have been interpreted as being due to *o*-, *m*-, and *p*-$CH_3C_6H_4^+$.[8] The phenylium ion structure for the $C_6H_5^+$ ion formed by loss of H_2 from protonated benzene has been supported by an elegant argument based on the conservation of orbital symmetry.[9]

We have not, however, found any data describing the gas-phase reactions of the phenylium ion. The report which follows contains several such reactions. In the course of ion–molecule reaction studies designed to shed light on the mechanism of radiation-induced protodehalogenation of halobenzenes,[10] a convenient source of phenylium ions was discovered which prompted this study of their ion–molecule reactions. The reactions of $C_6H_5^+$, with D_2, CH_4, CD_4, CH_3F, CH_3Cl, CH_3Br, CH_2Cl_2, C_2H_6, C_2H_4, propene, cyclopropane, C_6H_5Cl, and C_6H_5F, are reported here.

Experimental Section

The ion cyclotron resonance spectroscopic techniques employed in this study have been described in detail.[11] The experiments were performed with an ionizing electron energy just sufficient to produce the ions of interest (typically 16 to 20 eV). The total pressure in the reaction cell was 10^{-5} Torr. Double resonance experiments were carried out under strong field conditions[12] with an accelerating field of 0.7 V/cm. All gaseous reagents were purchased from Matheson Co. and used without further purification. Liquid reagents were purchased from standard commercial suppliers and purified by

---

* Address correspondence to this author at Washington University.

Gaspar et al. / Phenylium ($C_6H_5^+$) Ion-Molecule Reactions